Smart Structures and Systems, *Vol. 27, No. 2 (2021) 257-266*
DOI: https://doi.org/10.12989/sss.2021.27.2.257

Damage detection of bridge structures under unknown seismic excitations using support vector machine based on transmissibility function and wavelet packet energy

Lijun Liu [a], Jianan Mi [b], Yixiao Zhang [c] and Ying Lei*

School of Architecture and Civil Engineering, Xiamen University, Xiamen 365001, China

(*Received August 16, 2020, Revised October 12, 2020, Accepted December 10, 2020*)

Abstract. Since it may be hard to obtain the exact external load in practice, damage identification of bridge structures using only structural responses under unknown seismic excitations is an important but challenging task. Since structural responses are determined by both structural properties and seismic excitation, it is necessary to remove the effects of external excitation and only retain the structural information for structural damage identification. In this paper, a data-driven approach using structural responses only is proposed for structural damage alarming and localization of bridge structures. The transmissibility functions (TF) of structural responses are used to eliminate the influence of unknown seismic excitations. Moreover, the inverse Fourier transform of TFs and wavelet packet transform are used to reduce the influence of frequency bands and to extract the damage-sensitive feature, respectively. Based on Support vector machines (SVM), structural responses under ambient excitations are used for training SVM. Then, structural responses under unknown seismic excitations are also processed accordingly and used for damage alarming and localization by the trained SMV. The numerical simulation examples of beam-type bridge and a cable-stayed bridge under unknown seismic excitations are studied to illustrate the performance of the proposed approach.

Keywords: structural damage identification; unknown seismic excitation; transmissibility function; wavelet packet energy; support vector machine

1. Introduction

An increasing number of long-span bridges have been constructed with the rapid development of building material and engineering technology. However, these bridges in service may be seriously damaged and cause great economic loss under the strong earthquake. Therefore, the research of bridge structural damage identification technology has become an increasingly significant research topic (Fujino *et al*. 2005, Li *et al*. 2013, An *et al*. 2019, Tjen *et al*. 2020). In recent years, a large number of bridge structural damage identification methods based on dynamic characteristics have been proposed (Siringoringo and Fujino 2006, Kaloop and Li 2011, An *et al*. 2015, Xu *et al*. 2018). Generally speaking, the current approaches used to identify structural damage can be divided into two categories. The first one is based on the known or measured excitation and dynamic responses of the structure (Maia *et al*. 2003, Liu *et al*. 2009). The other one is only based on the monitored responses data of the structure (Noori *et al*. 2018, Yan *et al*. 2019). Compared to the first category of methods, the methods based on the responses only do not need the information of excitations as external excitations maybe unknown and difficult to be measured, e.g., wind and seismic excitations.

To eliminate the influence of unknown excitation, transmissibility function (TF) has attracted attentions and been utilized in damage identification of linear structural systems. TF-based methods can avoid the dependence on the system inputs, which are only used as the power sources and do not need to participate in the identification process. Maia *et al*. (2007) proposed the detection and relative damage quantification indicator (DRQ) as a reliable damage detection indicator, which was calculated through evaluating integral difference over a fixed frequency band between the intact transmissibility and damaged transmissibility. Maia *et al*. (2011) also developed a response vector assurance criterion (RVAC) for damage detection by considering the correlations of the TF. Chesné and Deraemaeker (2013) made a critical review of TF which highlighted the importance of the choice of the frequency bands and the dependency on the force location. Li *et al*. (2015) proposed a new method using the weighting factor to increase the weight of resonance. The proposed indicator had better performance than previous methods, but the frequency also needed to be chosen for each case. Zhu *et al*. (2015) proposed a decentralized structural damage detection procedure using TF. Zhou *et al*. (Zhou *et al*. 2015, 2016, Zhou and Wahab 2016, 2017) suggested combining the TF with the distance measure such as Mahalanobis

*Corresponding author, Ph.D., Professor,
E-mail: ylei@xmu.edu.cn
[a] Ph.D., Associate Professor, E-mail: liulj214@xmu.edu.cn
[b] Master Student, E-mail: mijianan@stu.xmu.edu.cn
[c] Master Student,
E-mail: 25320181152869@stu.xmu.edu.cn

http://www.techno-press.org/?journal=sss&subpage=7
ISSN: 1738-1584 (Print), 1738-1991 (Online)

distance to detect structural damage. Yan *et al*. (2019) recently presented a literature review that discussed existing studies on TF-based system identification. However, damage identification based on TF is greatly influenced by the choice of the frequency band, as inappropriate selection of frequency band may lead to wrong results. Besides, the TF-based indicator is not sensitive to minor local damage because Fourier transform is a global transformation (Fan *et al*. 2013).

Wavelet packet transform (WPT) has advantage over the traditional Fourier analysis of signals because of the time-frequency multi-resolution property, which makes WPT more sensitive to local damage (Noori *et al*. 2018). Therefore, WPT has been employed for structural damage identification and proved to be an effective method for obtaining damage features. Sun and Chang (2002) proved that the wavelet packet energy is sensitive to structural damage and can be used for damage assessment. Ren *et al*. (2008) studied a signal-based damage identification method using the wavelet packet energy changes to shear connectors as the damage feature. Based on wavelet transform, Young Noh *et al*. (2011) developed damage-sensitive features and theoretically derived the relationship between the wavelet energies and structural parameters. Jiang and Chen (2012) proposed a WPT component energy index to establish the slope vector and the curvature vector for damage detection. Yan and Li (2012) developed a new damage detection algorithm named natural excitation technique based on wavelet packet energy for the continuous beam. Wang and Shi (2018) proposed the energy curvature difference (ECD) index based on WPT to identify the damage in structures. Moreover, the strain data were transformed into a modified wavelet packet energy rate index to identify the damage location and severity in Noori *et al*. (2018). However, the above methods assumed the impulse excitation acting on the structures, which is not applicable when excitations are different before and after the damage occurs.

In this study, TF and WPT are fused to overcome their respective drawbacks. By using TF, the influence of external excitation is eliminated. Moreover, inverse Fourier transform of TF is conduced to obtain the virtual time domain signals, the frequency bands selection can be avoided. Besides, WPT is more sensitive to detailed local variation than global Fourier transform, so it is employed to decompose the virtual time domain signals to extract structural damage feature.

In recent years, data-driven and machine learning (ML) methods for structural health monitoring have received great research attentions. Bao *et al*. (2019) presented an excellent review on the state of the art of data science and engineering in structural health monitoring. Recently, Bao and Li (2020) have shared light on principles for machine learning (ML) paradigm for structural health monitoring with their pioneering methodologies and successful examples. Among the various ML approaches, support vector machine (SVM) has been widely accepted as effective tool for feature extraction and damage detection (Diao *et al*. 2018). SVM is a supervised learning technology based on Vapnik-Chervonenkis theory (Cortes and Vapnik 1995), which could overcome the shortcomings of neural networks such as local minimization and insufficient statistical ability. Moreover, SVM is especially suitable for small size samples (Luts *et al*. 2012). Gui *et al*. (2017) proposed three optimization algorithms for damage detection using SVM, in which two feature extraction methods based on time series data were selected to obtain effective damage features. Dushyanth *et al*. (2016) proposed a two-step method based on SVM that can significantly improve the estimation accuracy of defect locations. This method required relatively fewer training samples compared with the artificial neural network method. Diao *et al*. (2018) proposed a damage identification method based on TF and SVM, and adopted the offshore platform under white noise excitation as an example to prove its efficiency.

In this paper, a data-driven approach is proposed for detecting structural damage under unknown seismic excitations using SVM based on TF and wavelet packet energy. First, TF is used to remove the effects of different external excitations. Then, the inverse Fourier transform is implemented on the TFs to obtain the virtual time domain signal to further eliminate the influence of frequency bands. WPT, which has the ability to subtle damage information acquisition, is conducted on the virtual time domain signal to extract the features. Finally, the extracted features from structural responses under ambient excitations are used for training SVM, and the extracted features from structural responses under unknown seismic excitation are used for damage alarming and localization by the trained SMV. The numerical simulations of structural damaged identification of a beam-type bridge and a cable-stayed bridge under unknown seismic excitation are studied to validate the proposed approach.

2. Wavelet packet energy based on transmissibility functions

2.1 Transmissibility Function (*TF*)

TF is defined as the ratio between the Fourier transform of responses from two measurement points. Herein, TF under seismic excitation is studied. As for an *n*-DOFs system under seismic excitation $\ddot{x}_g(t)$, the motion equation can be described as:

$$\mathbf{M}\ddot{\mathbf{x}}(t) + \boldsymbol{C}\dot{\boldsymbol{x}}(t) + \boldsymbol{K}\boldsymbol{x}(t) = -\boldsymbol{MI}\ddot{x}_g(t) \tag{1}$$

where $\mathbf{M}$, $\mathbf{C}$, and $\mathbf{K}$ represent the mass, damping, and stiffness matrices of the system, respectively, $x(t)$ is the displacement response vector, $\mathbf{I}$ denotes the influence vector of seismic input. When the structural initial condition is static, the motion equation could be transformed to the frequency domain

$$(\mathbf{M}\omega^2 + \mathbf{C}\omega + \mathbf{K})\boldsymbol{x}(\omega) = -\mathbf{MI}\ddot{x}_g(\omega) \tag{2}$$

$$\begin{aligned} \boldsymbol{x}(\omega) &= \boldsymbol{H}(\omega)\mathbf{MI}\ddot{x}_g(\omega); \\ \boldsymbol{H}(\omega) &= -(\mathbf{M}\omega^2 + \mathbf{C}\omega + \mathbf{K})^{-1} \end{aligned} \tag{3}$$

Each line of the Eq. (3) in the frequency domain can be represented as

$$
\begin{aligned}
x_i &= H_{i1}(m_{11}I_1 + m_{12}I_2 + \cdots + m_{1n}I_n)\ddot{x}_g \\
&\quad + H_{i2}(m_{21}I_1 + m_{22}I_2 + \cdots + m_{2n}I_n)\ddot{x}_g + \cdots \\
&\quad + H_{in}(m_{n1}I_1 + m_{n2}I_2 + \cdots + m_{nn}I_n)\ddot{x}_g \\
&= \sum_{p=1}^{n} H_{i,p}(\omega) \sum_{q=1}^{n} m_{p,q} I_q \, \ddot{x}_g
\end{aligned} \tag{4}
$$

where m_{ij} is the $(i,j)^{\text{th}}$ element in matrix $\mathbf{M}$, I_i is i-th element in vector $\mathbf{I}$. The TF $T_{i,j}(\omega)$ can be calculated as

$$
\begin{aligned}
T_{i,j}(\omega) &= \frac{x_i(\omega)}{x_j(\omega)} = \frac{\sum_{p=1}^{n} H_{i,p}(\omega) \sum_{q=1}^{n} m_{p,q} I_q \, \ddot{x}_g}{\sum_{p=1}^{n} H_{j,p}(\omega) \sum_{q=1}^{n} m_{p,q} I_q \, \ddot{x}_g} \\
&= \frac{\sum_{p=1}^{n} H_{i,p}(\omega) \sum_{q=1}^{n} m_{p,q} I_q}{\sum_{p=1}^{n} H_{j,p}(\omega) \sum_{q=1}^{n} m_{p,q} I_q}
\end{aligned} \tag{5}
$$

where $x_i(\omega)$ and $x_j(\omega)$ are the outputs at DOF i and DOF j respectively; $H_{i,p}(\omega)$ and $H_{j,p}(\omega)$ are the frequency response functions at DOF i and DOF j when excitation at DOF p, respectively.

It can be noted that the $T_{i,j}(\omega)$ is not influenced by the seismic excitation $\ddot{x}_g(\omega)$. Therefore, the TF can eliminate the influence of different seismic excitations and only depends on the structural characteristics.

Moreover, the strain is more sensitive to the small deviation in the structural responses than displacement because it involves the second spatial derivative of displacement (Noori *et al.* 2018). Strain transmissibility which is defined as the ratio of strain response spectra has revealed a better performance compared to traditional transmissibility (Cheng *et al.* 2017). In this study, strain responses of two adjacent DOFs are used to calculate transmissibility. For beam element as shown in Fig. 1, the shape functions of the corresponding DOFs of beam element is $\{N\} = \{N_1 \quad N_2 \quad N_3 \quad N_4 \quad N_5 \quad N_6\}^T$ and $\{x_i\}$ is the corresponding displacements of element i. (u, v) denotes the location of a strain gauge deployed in the beam element, ε is the measured strain. The strain ε is proportional to curvature, and the TF $T_{i,j}^{\varepsilon}(\omega)$ of strain could be expressed as

$$
\begin{aligned}
T_{i,j}^{\varepsilon}(\omega) &= \frac{\varepsilon_i(\omega)}{\varepsilon_j(\omega)} = \frac{F[\varepsilon_i(t)]}{F[\varepsilon_j(t)]} = \frac{F[v \cdot \kappa_i(t)]}{F[v \cdot \kappa_j(t)]} \\
&= \frac{F[v \cdot (\{N\}^T\{x_i(t)\})'']}{F\left[v \cdot \left(\{N\}^T\{x_j(t)\}\right)''\right]} \\
&= \frac{v \cdot (\{N\}^T)'' F[\{x_i(t)\}]}{v \cdot (\{N\}^T)'' F[\{x_j(t)\}]} = \frac{(\{N\}^T)''\{x_i(\omega)\}}{(\{N\}^T)''\{x_j(\omega)\}}
\end{aligned} \tag{6}
$$

where $F[\cdot]$ denotes the Fourier transform, κ is the curvature, which is also the second derivative of deflection, v is the distance from the surface to the central axis as depicted in Fig. 1. Same as the TF of displacements in Eq. (5), $T_{i,j}^{\varepsilon}(\omega)$ is not influenced by the seismic excitation $\ddot{x}_g(\omega)$. Moreover, the TF $T_{i,j}^{\varepsilon}(\omega)$ of strain is directly related to structural health state since $\frac{x_i(\omega)}{x_j(\omega)} = T_{i,j}(\omega)$ is the function of frequency response functions as Eq. (5) represents.

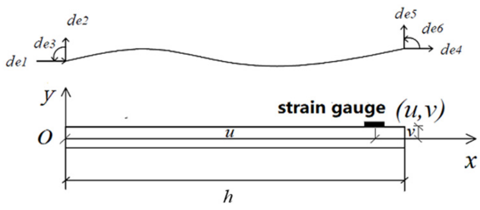

Fig. 1 Strain in the beam element

For a structure with n measurement points, a 1×(n-1) vector can be obtained

$$
\begin{aligned}
&\boldsymbol{T}^{\varepsilon}(\omega) \\
&= \left\{T_{1,2}^{\varepsilon}(\omega), T_{2,3}^{\varepsilon}(\omega), T_{3,4}^{\varepsilon}(\omega), \cdots, T_{n-2,n-1}^{\varepsilon}(\omega), T_{n-1,n}^{\varepsilon}(\omega)\right\}
\end{aligned} \tag{7}
$$

After TF has been obtained, the inverse Fourier transform of TF is conducted to obtain the virtual time domain signal, namely $\bar{\boldsymbol{T}}(t)$.

$$
\begin{aligned}
\bar{\boldsymbol{T}}(t) &= F^{-1}[\boldsymbol{T}^{\varepsilon}(\omega)] \\
&= \{\bar{T}_{1,2}(t), \bar{T}_{2,3}(t), \cdots, \bar{T}_{m,m+1}(t), \cdots, \\
&\quad \bar{T}_{n-2,n-1}(t), \bar{T}_{n-1,n}(t)\}
\end{aligned} \tag{8}
$$

2.2 Wavelet packet energy (WPE)

WPT can be regarded as the extension of the wavelet transform, which can decompose a signal level-by-level. The essence of WPT is to pass the signal through a set of high and low frequency filters, and every time of decomposition divides the signal into low frequency and high frequency components. In this way, after j times of decomposition, the original signal will get 2^j wavelet packet components, and the frequency of the signal is also divided into 2^j segments. Thus, the WPE of different frequency bands can be obtained. The WPE of the vibration signal in each frequency band represents the vibration characteristic information of the original signal, and this energy is very sensitive to structural damage. Therefore, the WPE of each frequency band could be used as the damage sensitive feature.

As mentioned before, due to the global nature of the Fourier transform, TF is not sensitive to slight local damage. But WPT can reflect the local characteristics of signals both in the time domain and frequency domain for the characteristic of multi-scale and adjustable window focus. To overcome the limitations of TF, WPE based on TF is proposed in this study, which could eliminate the influence of excitation and frequency band, and is sensitive to local damage.

Then WPT is utilized to decompose the virtual time domain signal $\bar{T}_{m,m+1}(t)$ to get wavelet packet energy as a damage feature. 2^j wavelet packet components are obtained after j levels of decomposition

$$
\bar{T}_{m,m+1}(t) = \sum_{i=0}^{2^j-1} \bar{T}_{m,m+1}^{i,j}(t) \tag{9}
$$

where $\bar{T}^{i,j}_{m,m+1}(t)$ is the wavelet packet component signal, the energy of each wavelet packet component can be expressed as

$$E^{i,j}_{m,m+1} = \int_{-\infty}^{\infty} \bar{T}^{i,j}_{m,m+1}(t)^2\, dt \tag{10}$$

For time domain signal $\bar{T}_{m,m+1}(t)$, a 1×2^j vector can be obtained

$$\boldsymbol{E}_{m,m+1} = \left\{E^{0,j}_{m,m+1}, E^{1,j}_{m,m+1}, E^{2,j}_{m,m+1}, \cdots, E^{2^j-1,j}_{m,m+1}\right\} \tag{11}$$

$$\delta_{m,m+1} = \left\|\mathbf{E}_{m,m+1} - \bar{\mathbf{E}}_{m,m+1}\right\| \tag{12}$$

where $\| \quad \|$ means the module of the vector, $\bar{\mathbf{E}}_{m,m+1}$ is the WPE result of the intact structure.

Thus, the virtual time domain signal $\bar{T}_{m,m+1}(t)$, obtained by the inverse Fourier transform of TF between two adjacent strain responses in the structure, is decomposed by WPT to derive the WPE vector $\boldsymbol{E}_{m,m+1}$. Then, $\delta_{m,m+1}$ means the WPE differences between the structure to be identified and the intact structure. If $\delta_{m,m+1}$ is closed to zero, it means there is no damage between these two adjacent points of the structure. If $\delta_{m,m+1}$ changes a lot, it means the existence of structural damage. Considering a structure with n measurement points, a $1 \times (n-1)$ vector can be acquired as follows

$$\boldsymbol{\delta} = \left\{\delta_{1,2}, \delta_{2,3}, \cdots, \delta_{m,m+1}, \cdots, \delta_{n-2,n-1}, \delta_{n-1,n}\right\} \tag{13}$$

in which δ represents the wavelet packet energy difference in the structure level. Therefore, when the energy differences of all adjacently measured points are close to zero, it indicates that the structure is undamaged. Otherwise, the structure is damaged. Herein, the vector δ is employed as the input of SVM for damage alarming.

As for the damage localization, a vector $\Delta_{m,m+1}$ is defined as

$$\Delta_{m,m+1} = \mathbf{E}_{m,m+1} - \bar{\mathbf{E}}_{m,m+1} \tag{14}$$

$\Delta_{m,m+1}$ in Eq. (14) reveals the difference of wavelet packet energy in the element level, between the structure to be identified and the intact structure. If this wavelet packet energy difference is very small, it indicates that the element is undamaged. Otherwise, the element is damaged. Therefore, the vector $\Delta_{m,m+1}$ is used as the input of SVM for damage localization.

3. Support vector machine (SVM)

SVM was first used for classification and then successfully extended to regression analysis by Cherkassky (1997). The basic idea of SVM is to construct an optimal separating hyperplane by maximizing the boundary between two types of data in space and minimizing misclassification. This section briefly introduces the basics of SVM.

The whole process of the SVM is illustrated in Fig. 2. Given the training sample set as $D = \{(\boldsymbol{x}_1, y_1), (\boldsymbol{x}_2, y_2), \ldots, (\boldsymbol{x}_m, y_m)\}$, $y_i \in \{-1, +1\}$. $\boldsymbol{x}_i$ represents the attributes contained in a sample, y_i represents the corresponding category label.

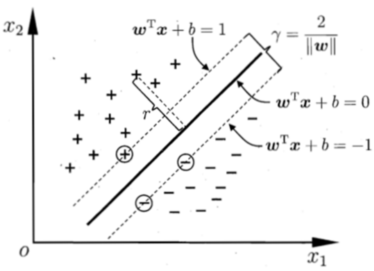

Note. $\boldsymbol{w}$: normal vector; $\boldsymbol{b}$: displacement term; γ: maximum margin; r: distance from the sample to the hyperplane

Fig. 2 Support vector and margin

The basic idea of classification learning is to find a classification hyperplane in the sample space based on the training sample set, and separate different samples.

SVM searches for the hyperplane which has the best generalization ability with the largest margin under the constraints of correct classification. The optimization of the solution can be expressed as

$$\min_{\boldsymbol{w},b} \frac{1}{2}\|\boldsymbol{w}\|^2 + C\sum_{i=1}^{N}\xi_i \tag{15a}$$

$$\text{Subject to } y_i\left((\boldsymbol{w}^T\boldsymbol{x}_i)+\text{b}\right) \ge 1-, \quad \xi_i \ge 0, \text{i}=1,2,\ldots,m. \tag{15b}$$

where ξ_i is the slack variable and C is the penalty factor. By Lagrange multipliers algorithm to solve the dual optimization problem as shown in Eq. (14), the nonlinear decision function will be yielded

$$f(x) = sign\left(\sum_{i=1}^{N}\alpha_i y_i K(\boldsymbol{x}, \boldsymbol{x}_i) + b\right), \quad \alpha_i > 0 \tag{16}$$

where $K(\boldsymbol{x}, \boldsymbol{x}_i)$ is defined as the kernel function. $sign$ is a sign function, its function is to take the positive and negative in parentheses. α_i is the Lagrange multiplier. By using this kernel function, it can analyze higher dimensional data.

Library for Support Vector Machines (LIBSVM) is a simple, fast and effective software package for SVM classification and regression developed by Professor Lin Chih-Jen of Taiwan University (Chang and Lin 2001). Selecting a suitable penalty factor and kernel function parameter for the SVM could enhance their accuracy for damage classification (Diao *et al*. 2018).

Regarding the optimal selection of SVM parameters, there is no recognized best method in the world. The Gaussian radial basis function $K(x, x_i) = \exp\left(-gamma\|x - x_i\|^2\right)$ is selected as the kernel function. Grid parameter optimization is used to find the penalty factor C and the kernel function parameter g ($gamma$) in the numerical example. To effectively estimate the accuracy of the models, the Cross-validation (CV) procedure is adopted, which could also prevent the overfitting problem (Gui *et al*. 2017).

In summary, the flow of the proposed approach is shown in Fig. 3. In the structural damage alarming stage, only structural responses of undamaged structure under the ambient excitation are needed in the training set. The measured strain responses are processed through the transmissibility function, inverse Fourier transform, and wavelet packet energy by Eqs. (7)-(8) and Eq. (11) and Eq. (13), subsequently. Then, the vector δ in Eq. (13) is used as the input of SVM model 1 for training. When the structure is subjected to the unknown seismic excitation, the measured strain responses are processed in the same way, and the damage alarming could be predicted by trained SMV model 1. In the damage localization stage, only structural ambient responses of undamaged structure and damaged structure with a single-level one element damaged are required in the training set. The measured strain responses are processed by Eqs. (7)-(8) and Eq. (11) and Eq. (14), subsequently and the vector $\Delta_{m,m+1}$ is used as the inputs of SVM model 2 for training. When the structure is subjected to the unknown seismic excitation, the measured strain responses are processed in the same way, and the damage localization can be predicted by trained SMV model 2.

It should be noted that if researchers know the suspicious area of damaged elements based on engineering experience, only the strains in the suspicious area should be measured. Otherwise, the strains of all elements should be measured to conduct damage localization. The recently developed distributed strain sensing such as long-gauge strain technology can solve the above problem (Huang and Wu 2017), and the application of long-gauge strain should be investigated in the future.

4. Numerical simulations

The structure simulations of a simply supported beam and a real bridge model are carried out to demonstrate and verify the proposed approach in this section.

4.1 Numerical simulation of the simply supported beam

First, a linear and statically determined beam under seismic excitation is taken as an example, as shown in Fig. 4. The length of the beam is 2.8 m. The moment of inertia is $I = 1.4 \times 10^{-8}\ m^4$, Young's modulus of elasticity is $E = 206\ GPa$ and the mass density is $\rho = 7800\ kg/m^3$. The beam is divided into 28 elements. The strain responses from element 9 to element 20 (the middle span of the beam, total 12 elements) are measured while the sampling frequency is 2000 Hz and the duration lasts 5 s. The strain was observed at 3/4 length on the upper surface of each element. Measurement noise is considered here. The Gaussian distributed noise with 5% standard deviation to the signals is added to the "measurement" data. Different damage levels simulation is achieved by reducing the stiffness of the beam element. Based on the experimental analysis, the strain responses are decomposed to level 3 with Db20

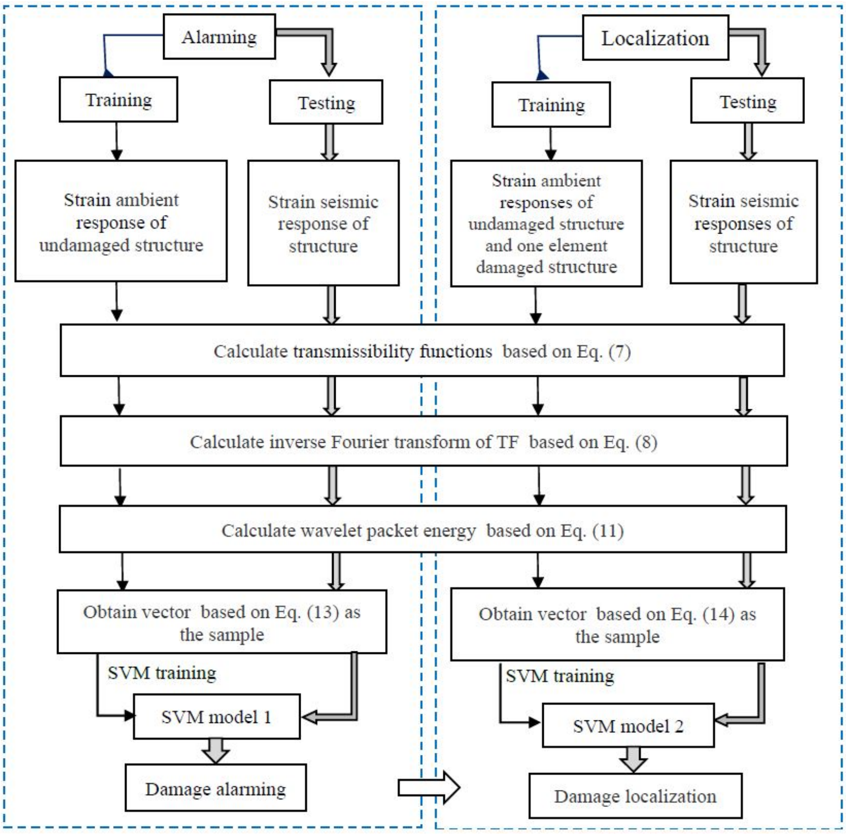

Fig. 3 Flowchart of damage identification approach

Fig. 4 The finite element model of the simply supported beam

wavelet in this study, which has revealed a better performance, and 8 component energies are generated in total.

4.1.1 Damage alarming

For the training set, ambient excitations act on every vertical DOF of the undamaged beam. For a total of 12 elements (element 9 to element 20), a 11-element vector δ can be obtained by Eq. (13). The entire training set includes only 50 structural ambient responses from the undamaged structure. The test set consists of three working conditions: undamaged, single- element damaged and multi- element damaged. Seismic excitations of El-Centro earthquake (1940, USA) and Kobe-Takatori earthquake (1995, Japan) are employed in the test set. It is assumed that the earthquake excitations act on every vertical DOF as the

Table 1 Damage conditions and predicted results of damage alarming (testing set)

Test number	1	2	3	4	5	6	7	8	9	10	11	12
DE	-	11	12	13	14	15	16	10,12	10,13	10,14	10,15	10,16
DL (%)	-	15	15	20	20	25	25	20,25	20,25	20,25	20,25	20,25
El-Centro	1	1*	1*	-1	-1	-1	-1	-1	-1	-1	-1	-1
Kobe-Takatori	1	-1	-1	-1	-1	-1	-1	-1	-1	-1	-1	-1

Note. DE: damage element; DL: damage level; 1: undamaged; -1: damaged; *misclassification

Table 2 Damage conditions and predicted results of damage location

	DE	DL (%)	Δ9,10	Δ10,11	Δ11,12	Δ12,13	Δ13,14	Δ14,15	Δ15,16	Δ16,17	Δ17,18	Δ18,19	Δ19,20
	-	-	1	1	1	1	1	1	1	1	1	1	1
	11	15	1	1*	**-1**	1	1	1	1	1	1	1	1
	12	15	-1*	1	1*	**-1**	1	1	1	1	1	1	1
	13	20	1	1	1	1*	**-1**	1	1	1	1	1	1
	14	20	1	1	1	1	1*	**-1**	1	1	1	1	1
El-Centro	15	25	-1*	1	1	1	1	**-1**	**-1**	1	1	1	1
	16	25	1	1	1	1	1	1	**-1**	**-1**	1	1	1
	10,12	20,25	**-1**	**-1**	**-1**	**-1**	1	1	1	1	1	1	1
	10,13	20,25	**-1**	**-1**	1	**-1**	**-1**	1	1	1	1	1	1
	10,14	20,25	**-1**	**-1**	1	1	**-1**	**-1**	1	1	1	1	1
	10,15	20,25	**-1**	**-1**	1	1	1	**-1**	**-1**	1	1	1	1
	10,16	20,25	**-1**	**-1**	1	1	1	1	**-1**	**-1**	1	1	-1*
	-	-	1	1	1	1	1	1	1	1	1	1	1
	11	15	1	1*	**-1**	1	1	1	1	1	1	1	1
	12	15	1	1	1*	**-1**	1	1	1	1	1	1	1
	13	20	1	1	1	1*	**-1**	1	1	1	1	1	1
	14	20	1	1	1	1	1*	**-1**	1	1	1	1	1
Kobe-Takatori	15	25	1	1	1	1	1	**-1**	**-1**	1	1	1	1
	16	25	1	1	1	1	1	1	**-1**	**-1**	1	1	1
	10,12	20,25	**-1**	**-1**	**-1**	**-1**	1	1	1	1	1	1	1
	10,13	20,25	**-1**	**-1**	-1*	**-1**	**-1**	1	1	1	1	1	1
	10,14	20,25	**-1**	**-1**	1	1	**-1**	**-1**	1	1	1	1	1
	10,15	20,25	**-1**	**-1**	1	1	1	**-1**	**-1**	1	1	1	1
	10,16	20,25	**-1**	**-1**	1	1	-1*	1	**-1**	**-1**	1	1	1

Note. DE: damage element; DL: damage level; 1: undamaged; -1: damaged; *misclassification; Δ: obtained based on Eq. (14)

ambient excitations in the training set. The single-element damage includes damage locations at elements 11-16, with damage degree of 15%, 20% and 25%, respectively. The multi-element damaged condition includes damage location at elements (10,12), (10,13), (10,14), (10,15) and (10,16), with damage degree of 20% and 25%, respectively. There are 24 damage scenarios in total.

Table 1 displays the damage scenarios and predicted the results of the test set. Classification accuracy is used as the evaluation index. The one-class SVM module in LIBSVM is used for damage alarming when the training set contains only one type of label. The comparison between the predicted results and the real values under different earthquakes shows that the accuracy on the test set is 91.67% (22/24). Most of the classifications are accurate even if the training set only include response samples from the undamaged beam.

4.1.2 Damage localization

For each element, a 1 × 8 vector Δ in Eq. (14) can be acquired as the sample. The training set in the damage localization includes the undamaged condition and single-element damaged condition. Fifty ambient responses of the undamaged structure and five ambient responses of single-element damaged structure are used. Herein, it is assumed that only element 11 is damaged and the damage level is 25%, the percentage refers to stiffness reduction. Thus, the entire training set includes 50 + 5 = 55 samples.

Seismic excitations of El-Centro earthquake and Kobe-Takatori earthquake are employed in the test set. The test set includes the undamaged, single-element damaged and multi-element damaged conditions. In the single-element damaged condition, it is assumed that there is a total of 6 damaged locations (element 11 – element 16) with 3 damage levels (15%, 20% and 25%). In the multi-element damaged condition, it is assumed that there are total of 5 damaged elements combinations ((10, 12), (10, 13), (10, 14), (10, 15), (10, 16)) with damage degree of 20% and 25%, respectively. There are 24 damage conditions in total and 264 samples are used as the test set.

Table 2 displays the damage conditions and predicted the results of the test set. Samples containing damaged elements should be identified as damage (-1). For example, when element 15 is damaged with a degree of 25%, the vector $\Delta_{14,15}$ and $\Delta_{15,16}$ should be identified as damage (-1) and others Δ under the same damaged condition should be identified as undamaged (1). The comparison between the predicted results and the real values under different earthquakes shows the accuracy on the test set is 95.08% (251/264). Classification accuracy is used as the evaluation index. The most of the classifications are accurate even if the damage element and damage level of the training set and test set are different.

4.2 Numerical simulation example of a cable-stayed bridge

To further prove the robustness and effectiveness of the proposed method, the benchmark model of Haiwen bridge is used for numerical verification, which is a single tower cable-stayed bridge and located in Hainan province of China. The 2D benchmark model shown in Fig. 5 is provided by Tongji University, China. Only the main bridge section is considered, and the length of the girder is 460 m (230 m + 230 m). The structural parameters are set as: the moment of inertia is $I = 2.326\,m^4$, Young's modulus of elasticity is $E = 210\,GPa$, and the mass of unit length is $\bar{m} = 17555\,kg/m$. The girder is divided into 236 elements. The sampling frequency is 2000 Hz and the duration is 10 s. The strain was observed at 3/4 length on the upper surface of each element. Only the linear behavior range of the structure is studied here. The connection between the bridge tower and the foundation is regarded as consolidation, which restricts all degrees of freedom. The two ends of the main beam are regarded as hinged joints which restricts the degrees of freedom of vertical and horizontal degrees of freedom. The connection of the main beam and the bridge tower is achieved by coupling the degrees of freedom of corresponding joints. The effects of asynchronous seismic excitation, soil-structure interaction and the nonlinear behavior of cables or bridge on damage detection have been neglected. It is assumed that both the seismic and ambient excitation acts on every vertical DOF of the structure. The linear analysis is run for calculation. The modal response history analysis is conducted to obtain the response. Gaussian noise with 5% standard deviation to the signals is added to the "measurement" data. Different damage levels are achieved by reducing the stiffness of the girder element.

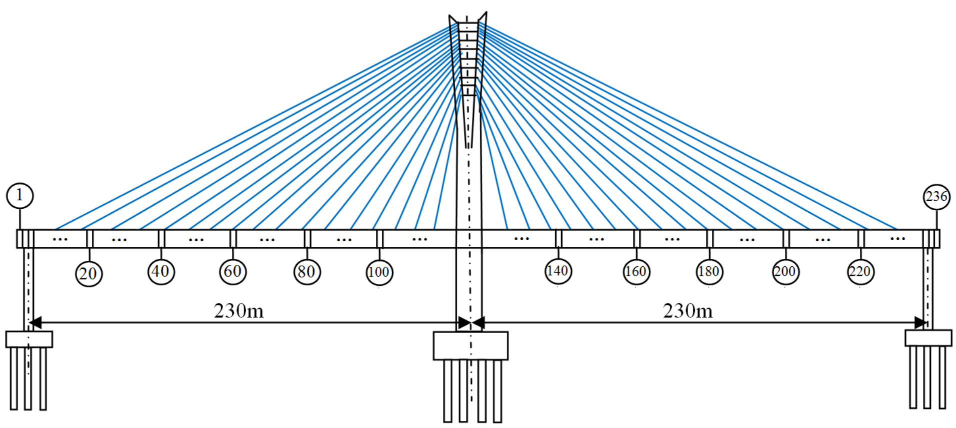

Fig. 5 The 2D model of the cable-stayed bridge

Table 3 Damage conditions and predicted results of damage alarming

Test number	1	2	3	4	5	6	7	8	9	10
DE	-	56	57	58	59	51,55	51,56	51,57	51,58	51,59
DL (%)	-	15	18	22	25	18,22	18,22	18,22	18,22	18,22
El-Centro	1	1*	-1	-1	-1	-1	-1	-1	-1	-1
Kobe-Takatori	1	-1	-1	1*	-1	-1	-1	-1	-1	-1

Note. DE: damage element; DL: damage level; 1: undamaged; -1: damaged; *misclassification

Table 4 Damage conditions and predicted results of damage location

	DE	DL (%)	Δ50,51	Δ51,52	Δ52,53	Δ53,54	Δ54,55	Δ55,56	Δ56,57	Δ57,58	Δ58,59	Δ59,60
	-	-	1	1	1	1	1	1	1	1	1	1
	56	15	1	1	1	1	1	**-1**	1*	1	1	1
	57	18	1	1	1	1	1	1	**-1**	**-1**	1	1
	58	22	1	1	1	1	1	1	1	**-1**	**-1**	1
El-Centro	59	25	1	1	1	1	1	1	1	1	**-1**	**-1**
	51,55	20,25	**-1**	**-1**	1	1	**-1**	**-1**	1	1	1	1
	51,56	20,25	**-1**	**-1**	1	1	1	**-1**	**-1**	1	1	1
	51,57	20,25	**-1**	**-1**	1	1	1	1	**-1**	**-1**	1	1
	51,58	20,25	**-1**	**-1**	1	1	1	1	1	**-1**	**-1**	1
	51,59	20,25	**-1**	**-1**	1	1	1	1	1	1	**-1**	**-1**
	-	-	1	1	1	1	1	1	1	1	1	1
	56	15	1	1	1	1	1	**-1**	1*	1	1	1
	57	18	1	1	1	1	1	1	**-1**	**-1**	1	1
	58	22	1	1	1	1	1	1	1	**-1**	**-1**	1
Kobe-Takatori	59	25	1	1	1	1	1	1	1	1	**-1**	**-1**
	51,55	20,25	**-1**	**-1**	1	1	**-1**	**-1**	1	1	1	1
	51,56	20,25	**-1**	**-1**	1	1	1	**-1**	**-1**	1	1	1
	51,57	20,25	**-1**	**-1**	1	1	1	1	**-1**	**-1**	1	1
	51,58	20,25	**-1**	**-1**	1	1	1	1	1	**-1**	**-1**	1
	51,59	20,25	**-1**	**-1**	1	1	1	1	1	1	**-1**	**-1**

Note. DE: damage element; DL: damage level; 1: undamaged; -1: damaged; *misclassification; Δ: obtained based on Eq. (14)

Based on the experimental analysis, the strain responses are decomposed to level 3 with Db20 wavelet in this study, which has revealed a better performance, and 8 component energies are generated in total.

4.2.1 Damage alarming

The partial strain responses (from element 50 to element 80) are measured in this bridge. For a total of 31 elements, a 30-element vector δ can be obtained by Eq. (13). The entire training set includes only 50 structural ambient responses from the undamaged structure. The test set also consists of three working conditions similar to example 1. Seismic excitations of the El-Centro earthquake and Kobe-Takatori earthquake are employed in the test set. It is assumed that the earthquake excitations and the ambient excitations both act on every vertical DOF. The single-element damage includes damage locations at elements 56-59, with damage degrees of 15%, 18%, 22% and 25%, respectively. The multi-element damaged condition includes damage locations at elements (51,55), (51,56), (51,57), (51,58), (51,59), with damage degrees of 18% and 22%, respectively. There are 20 damage scenarios in total.

Table 3 displays the damage scenarios and predicted the results of the test set. The comparison between the predicted results and the real values under different earthquakes shows the accuracy on the test set is 91.67% (22/24). It can be seen that most of the classifications are accurate even if the training set only included response samples from the undamaged beam.

4.2.2 Damage localization

Similarly, for each element, a 1×8 vector Δ in Eq. (14) can be acquired as the sample. The training set in the damage localization includes the undamaged and single-element damaged conditions. Fifty ambient responses of the undamaged structure and five ambient responses of single-element damaged structure are used. It is assumed that only element 50 is damaged with the damage level 25%. Thus, the entire training set includes 55 samples.

Seismic excitations El-Centro and Kobe-Takatori earthquake are employed in the test set. Three working conditions of the test set in damage localization are similar to the one in damage alarming. So, there are 20 damage conditions and 200 samples are used as the test set.

Table 4 displays the damage conditions and predicted the results of the test set. The comparison between the predicted results and the real values under different earthquakes shows that the accuracy on the test set is 99% (198/200).

5. Conclusions

In this paper, a novel data-driven approach is proposed for detecting bridge damage under unknown seismic excitation. TF and WPT are fused to extract damage features effectively. Since only the liner behavior of the structure is investigated here, the utilization of TF based on structural responses can eliminate the effects of different seismic excitations on structural responses. Then, the inverse Fourier transform of the TF is implemented to obtain the virtual time domain signals, so the frequency bands selection in previous TF based damage detection is avoided. Moreover, WPT is adopted to decompose the virtual time domain signal to acquire the wavelet packet energy. The wavelet packet energy difference compared to the intact structure are taken as the inputs of two support vector machines to accomplish damage alarming and localization, respectively. The numerical simulation of damage identification of bridge under unknown seismic excitations have proved that the proposed approach can accomplish damage alarming and localize the single or multiple element damage in structure with satisfaction.

It is noted that only ambient responses of the undamaged structure are needed to train SVM for damage alarming. For damage localization, only ambient responses of undamaged structure and a single-element damaged structure with just one damage level are required to train SVM. Therefore, the proposed approach is suitable for engineering applications.

However, for the damage quantification, it is still required to use structural responses from structures with different damaged elements and various damage degrees to train the SVM. Such data are hard to acquire in practice. Therefore, it needs further investigation for damage quantification using SVM. Furthermore, the detection of nonlinear behaviors should be studied since the bridge structure tends to reveal nonlinear behaviors under strong seismic excitations.

Acknowledgments

The research in this paper is supported by the National Key R&D Program of China via Grant No. 2017YFC1500603. The authors thank Associate Prof. Ye Xia at Tongji University for providing the benchmark model of Haiwen bridge.

References

An, Y.H., Spencer, B.F. and Ou, J.P. (2015), “A Test method for damage diagnosis of suspension bridge suspender cables”, *Comput.-Aided Civil Infrastruct. Eng.*, **30**(10), 771-784. https://doi.org/10.1111/mice.12144

An, Y.H., Chatzi, E., Sim, S.H., Laflamme, S., Blachowski, B. and Ou, J.P. (2019), “Recent progress and future trends on damage identification methods for bridge structures”, *Struct. Control Health Monitor.*, **26**(10), e2416. https://doi.org/10.1002/stc.2416

Bao, Y. and Li, H. (2020), “Machine learning paradigm for structural health monitoring”, *Struct. Health Monitor.* https://doi. org/10.1177/1475921720972416

Bao, Y.Q., Chen, Z., Wei, S., Xu, Y., Tang, Z. and Li, H. (2019), “The state of the art of data science and engineering in structural health monitoring”, *Eng.*, **5**(2), 234-242. https://doi.org/10.1016/j.eng.2018.11.027

Chang, C.C. and Lin, C.J. (2001), “LIBSVM: a library for support vector machines”. http://www.csie.ntu.edu.tw/cjlin/papers/ guide/data

Cheng, L., Busca, G., Roberto, P., Vanali, M. and Cigada, A. (2017), “Damage Detection Based on Strain Transmissibility for Beam Structure by Using Distributed Fiber Optics”, *Proceedings of the Society for Experimental Mechanics Series*, Volume 7, pp. 27-40. https://doi.org/10.1007/978-3-319-54109-9_4

Cherkassky, V. (1997), “The nature of statistical learning theory”, *IEEE Transact. Neural Networks*, **8**(6), 1564-1564. https://doi.org/10.1007/978-1-4757-2440-0

Chesné, S. and Deraemaeker, A. (2013), “Damage localization using transmissibility functions: A critical review”, *Mech. Syst. Signal Process.*, **38**(2), 569-584. https://doi.org/10.1016/j.ymssp.2013.01.020

Cortes, C. and Vapnik, V. (1995), “Support-vector networks”, *Mach. Learn*, **20**(3), 273-297. https://doi.org/10.1023/A:1022627411411

Diao, Y., Men, X., Sun, Z., Guo, K. and Wang, Y. (2018), “Structural Damage Identification Based on the Transmissibility Function and Support Vector Machine”, *Shock Vib.*, 1-13. https://doi.org/10.1155/2018/4892428

Dushyanth, N.D., Suma, M.N. and Latte, M.V. (2016), “Detection and localization of damage using empirical mode decomposition and multilevel support vector machine”, *Appl. Phys. A*, **122**(3). https://doi.org/10.1007/s00339-016-9753-z

Fan, Z., Feng, X. and Zhou, J. (2013), “A novel transmissibility concept based on wavelet transform for structural damage detection”, *Smart Struct. Syst., Int. J.*, **12**(3), 291-308. https://doi.org/10.12989/sss.2013.12.3_4.291

Fujino, Y., Kikkawa, H., Namikawa, K. and Mizoguchi, T. (2005), “Seismic retrofit design of long-span bridges on metropolitan expressways in Tokyo”, *Transport. Res. Record: J. Transport. Res. Board*, **11**, 335-342. https://doi.org/10.3141/trr.11s.1371l823v02811m0

Gui, G., Pan, H., Lin, Z., Li, Y. and Yuan, Z. (2017), “Data-driven support vector machine with optimization techniques for structural health monitoring and damage detection”, *KSCE J. Civil Eng.*, **21**(2), 523-534. https://doi.org/10.1007/s12205-017-1518-5

Huang, H. and Wu, Z.S. (2017), “Monitoring and structural analysis of a rehabilitated box girder bridge based on long-gauge strain sensors”, *Struct. Health Monitor.*, **17**(3), 586-597. https://doi:10.1016/j.engstruct.2015.04.024

Jiang, Z.G. and Chen, B. (2012), “Performance Degradation

Assessment of a Beam Structure by Using Wavelet Packet Energy", *Appl. Mech. Mater.*, **166-169**, 1102-1107. https://doi.org/10.4028/www.scientific.net/AMM.166-169.1102

Kaloop, M.R. and Li, H. (2011), "Sensitivity and analysis GPS signals based bridge damage using GPS observations and wavelet transform", *Measurement*, **44**(5), 927-937. https://doi.org/10.1016/j.measurement.2011.02.008

Li, H., Tao, D.W., Huang, Y. and Bao, Y.Q. (2013), "A data-driven approach for seismic damage detection of shear-type building structures using the fractal dimension of time-frequency features", *Struct. Control Health Monitor.*, **20**(9), 1191-1210. https://doi.org/10.1002/stc.1528

Li, X.Z., Peng, Z.K., Dong, X.J., Zhang, W.M. and Meng, G. (2015), "A new transmissibility based indicator of local variation in structure and its application for damage detection", *Shock Vib.*, 1-18. https://doi.org/10.1155/2015/850286

Liu, X., Lieven, N.A.J. and Escamilla-Ambrosio, P.J. (2009), "Frequency response function shape-based methods for structural damage localization", *Mech. Syst. Signal Process.*, **23**(4), 1243-1259. https://doi.org/10.1016/j.ymssp.2008.10.002

Luts, J., Molenberghs, G., Verbeke, G., Van Huffel, S. and Suykens, J.A.K. (2012), "A mixed effects least squares support vector machine model for classification of longitudinal data", *Computat. Statist. Data Anal.*, **56**(3), 611-628. https://doi.org/10.1016/j.csda.2011.09.008

Maia, N.M.M., Silva, J.M.M., Almas, E.A.M. and Sampaio, R.P.C. (2003), "Damage detection in structures: from mode shape to frequency response function methods", *Mech. Syst. Signal Process.*, **17**(3), 489-498. https://doi.org/10.1006/mssp.2002.1506

Maia, N.M.M., Ribeiro, A.M.R., Fontul, M., Montalvão, D. and Sampaio, R.P.C. (2007), "Using the detection and relative damage quantification indicator (DRQ) with transmissibility", *Key Eng. Mater.*, **347**, 455-460. https://doi.org/10.4028/www.scientific.net/KEM.347.455

Maia, N.M.M., Almeida, R.A.B., Urgueira, A.P.V. and Sampaio, R.P.C. (2011), "Damage detection and quantification using transmissibility", *Mech. Syst. Signal Process.*, **25**(7), 2475-2483. https://doi.org/10.1016/j.ymssp.2011.04.002

Noori, M., Wang, H., Altabey, W.A. and Silik, A.I. (2018), "A modified wavelet energy rate-based damage identification method for steel bridges", *Scientia Iranica*, **25**, 3210-3230. https://doi.org/10.24200/sci.2018.20736

Ren, W.-X., Sun, Z.-S., Xia, Y., Hao, H. and Deeks, A.J. (2008), "Damage identification of shear connectors with wavelet packet energy: laboratory test study", *J. Struct. Eng.*, **134**(5), 832-841. https://doi.org/10.1061/(ASCE)0733-9445(2008)134: 5(832)

Siringoringo, D.M. and Fujino, Y. (2006), "Experimental study of laser Doppler vibrometer and ambient vibration for vibration-based damage detection", *Eng. Struct.*, **28**(13), 1803-1815. https://doi.org/10.1016/j.engstruct.2006.03.006

Sun, Z. and Chang, C.C. (2002), "Structural Damage Assessment Based on Wavelet Packet Transform", *J. Struct. Eng.*, **128**(10), 1354-1361. https://doi.org/10.1061/(ASCE)0733-9445(2002)128:10(1354)

Tjen, J., Francesco, S. and Alessandro, D. (2020), "An entropy-based sensor selection approach for structural damage detection", *Proceedings of 2020 IEEE 16th International Conference on Automation Science and Engineering* (*CASE*).

Wang, P. and Shi, Q. (2018), "Damage Identification in Structures Based on Energy Curvature Difference of Wavelet Packet Transform", *Shock Vib.*, 1-13. https://doi.org/10.1155/2018/4830391

Xu, Y.L., Zhang, C.D., Zhan, S. and Spencer, B.F. (2018), "Multi-level damage identification of a bridge structure: a combined numerical and experimental investigation", *Eng. Struct.*, **156**, 53-67. https://doi.org/10.1016/j.engstruct.2017.11.014

Yan, P. and Li, Q. (2012), "Structural Damage Detection of Continuous Beam by NExT Based Wavelet Packet Energy", *Adv. Mater. Res.*, **490-495**, 2588-2593. https://doi.org/10.4028/www.scientific.net/AMR.490-495.2588

Yan, W.-J., Zhao, M.-Y., Sun, Q. and Ren, W.-X. (2019), "Transmissibility-based system identification for structural health Monitoring: Fundamentals, approaches, and applications", *Mech. Syst. Signal Process.*, **117**, 453-482. https://doi.org/10.1016/j.ymssp.2018.06.053

Young Noh, H., Krishnan Nair, K., Lignos, D.G. and Kiremidjian, A.S. (2011), "Use of wavelet-based damage-sensitive features for structural damage diagnosis using strong motion data", *J. Struct. Eng.*, **137**(10), 1215-1228. https://doi.org/10.1061/(ASCE)ST.1943-541X.0000385

Zhou, Y. and Wahab, M.A. (2016), "Rapid early damage detection using transmissibility with distance measure analysis under unknown excitation in long-term health monitoring", *J. Vibroeng.*, **20**(1), 823-831. https://doi.org/10.21595/jve.2016.19718

Zhou, Y.-L. and Wahab, M.A. (2017), "Cosine based and extended transmissibility damage indicators for structural damage detection", *Eng. Struct.*, **141**, 175-183. https://doi.org/10.1016/j.engstruct.2017.03.030

Zhou, Y.-L., Figueiredo, E., Maia, N., Sampaio, R. and Perera, R. (2015), "Damage detection in structures using a transmissibility-based Mahalanobis distance", *Struct. Control Health Monitor.*, **22**(10), 1209-1222. https://doi.org/10.1002/stc.1743

Zhou, Y.-L., Maia, N.M. and Abdel Wahab, M. (2016), "Damage detection using transmissibility compressed by principal component analysis enhanced with distance measure", *J. Vib. Control*, **24**(10), 2001-2019. https://doi.org/10.1177/1077546316674544

Zhu, D., Yi, X. and Wang, Y. (2015), "A local excitation and measurement approach for decentralized damage detection using transmissibility functions", *Struct. Control Health Monitor.*, **23**(3), 487*502. https://doi.org/10.1002/stc.1781